

MIT Open Access Articles

Inflammatory but not mitogenic contexts prime synovial fibroblasts for compensatory signaling responses to p38 inhibition

The MIT Faculty has made this article openly available. **Please share** how this access benefits you. Your story matters.

Citation: Jones, Douglas S. et al. "Inflammatory but Not Mitogenic Contexts Prime Synovial Fibroblasts for Compensatory Signaling Responses to P38 Inhibition." *Science Signaling* 11, 520 (March 2018): eaal1601 © 2018 The Authors

As Published: <http://dx.doi.org/10.1126/scisignal.aal1601>

Publisher: American Association for the Advancement of Science

Persistent URL: <http://hdl.handle.net/1721.1/117688>

Version: Author's final manuscript: final author's manuscript post peer review, without publisher's formatting or copy editing

Terms of Use: Article is made available in accordance with the publisher's policy and may be subject to US copyright law. Please refer to the publisher's site for terms of use.





Published in final edited form as:

Sci Signal. ; 11(520): . doi:10.1126/scisignal.aal1601.

Inflammatory but not mitogenic contexts prime synovial fibroblasts for compensatory signaling responses to p38 inhibition

Douglas S. Jones^{1,2}, Anne P. Jenney², Brian A. Joughin^{1,3}, Peter K. Sorger², and Douglas A. Lauffenburger^{1,*}

¹Department of Biological Engineering, Massachusetts Institute of Technology, Cambridge, MA, 02139

²Laboratory of Systems Pharmacology, HMS LINCS Center, Harvard Medical School, Boston, MA 02115

³Koch Institute for Integrative Cancer Biology, Massachusetts Institute of Technology, Cambridge, MA, 02139

Abstract

Rheumatoid arthritis (RA) is a chronic inflammatory disorder that causes joint pain, swelling, and loss of function. Development of effective new drugs has proven challenging, in part because of the complexities and interconnected nature of intracellular signaling networks, which complicate the effects of pharmacological interventions. Here, we characterized the signaling pathways that are activated in RA and evaluated the multivariate effects of targeted inhibitors. Synovial fluids from RA patients activated the kinase signaling pathways JAK, JNK, p38, and MEK in synovial fibroblasts (SFs), a stromal cell type that promotes RA progression. Kinase inhibitors enhanced signaling of “off-target” pathways in a manner dependent on stimulatory context. For example, p38 inhibitors, which have been widely explored in clinical trials for RA, resulted in undesirable increases in nuclear factor κ B (NF κ B), JNK, and MEK signaling in SFs in inflammatory, but not mitogenic, contexts. CREB, a transcription factor that functions in part within a negative feedback loop in MAPK signaling, emerged as a key regulator of this context-dependence. CREB activation was induced predominately by p38 in response to inflammatory stimuli but by MEK in response to mitogenic stimuli; the effects of drugs targeting p38 or MEK were therefore markedly different in SFs cultured in mitogenic or inflammatory conditions. Together these findings illustrate how stimulatory context can alter pathway cross-talk even for a fixed network topology, suggest cross-talk by p38 in inflammatory contexts limited the benefit of p38 inhibitors in RA, and furthermore demonstrate the need for careful consideration of p38-targeted drugs in inflammation-related disorders.

*Correspondence should be addressed to lauffen@mit.edu.

Author contributions: D.S.J. and A.P.J. performed the experiments; D.S.J. additionally performed the computational analyses; B.A.J. provided critical feedback, advice, and interpretations; D.S.J., P.K.S. and D.A.L. analyzed the results; and D.S.J., B.A.J., P.K.S. and D.A.L. wrote and edited the paper.

Competing interests: D.S.J is a current employee of Torque Therapeutics. All other authors have no competing interests to declare.

Introduction

Rheumatoid arthritis (RA) is an autoimmune disease characterized by inflammation and swelling of synovial joints, systemic complications, and significant morbidity and mortality (1–3). At the cellular level, autoantibodies and autoreactive T cells are believed to be responsible for initiation of RA (4, 5), while increasing evidence suggests synovial fibroblasts (SFs) – the resident fibroblast-like cells of the synovial membrane – play a critical role in perpetuating disease (6, 7). In healthy tissue SFs form a one to two cell-thick layer at the lining of the synovium, function to maintain the synovial membrane architecture, and produce lubricating molecules for the joint (8, 9). In RA; however, SFs have been described as transformed cells, in which they display morphologic features similar to cancer cells such as hyperplasia and resistance to apoptosis (6, 10). They also secrete various inflammatory cytokines and matrix degrading proteases (9, 11), including many of the most abundant cytokines in synovial fluids of RA patients (12). In addition, SF from RA patients (RA SF), but not SF from normal or osteoarthritis (OA) patients, are capable of invading and degrading human cartilage in immune-deficient mouse models of RA (13–15). The activated SF phenotype persists for several passages *ex vivo*, but RA SFs eventually adopt a more quiescent state following a few weeks in culture. Exposure to inflammatory cytokines such as IL-1 or TNF α can restore the activated state, suggesting SF activation in RA is dynamic and dependent upon inflammatory factors in the RA joint (10).

Biologic drugs targeting cytokines such as TNF α , IL-6, and IL-1, which mediate pro-inflammatory communication among the cells of the RA synovium, have improved disease management (16–20). However, resistance to treatment is a significant challenge, and fewer than 50% of patients remain in remission for one year (21). The FDA approval of tofacitinib (Xeljanz®), a small molecule inhibitor of the Janus kinases (JAKs), for RA demonstrates the therapeutic potential for targeting the kinases that regulate cytokine signaling and has brought promise for effective new therapies (22). However, drugs targeting other kinase pathways such as p38, MEK, and Syk have been met with limited success in clinical trials (23, 24). P38 inhibitors, in particular, received considerable interest from the pharmaceutical industry due to their ability to reduce inflammatory cytokine secretion in pre-clinical models but failed to show meaningful efficacy in clinical trials (23, 25). Drugs targeting p38 are no longer being developed for RA, but remain of interest for other inflammation-related disorders (25). Much of the negative clinical trial data for RA has not been published publicly (25), which limits the ability to both fully understand the reasons for their lack of clinical efficacy and to apply this learning to ongoing exploration of p38 inhibition in other inflammatory disorders. Their failure in RA, however, is thought to be based at least in part on an incomplete understanding of the effects of kinase-targeted drugs on complex, interconnected intracellular signaling networks, particularly as influenced by the complex inflammatory microenvironment in RA.

In this study, we combined high-throughput experimentation and data-driven modeling to explore inflammatory signaling responses of SFs and to evaluate the multivariate effects of specific kinase inhibitors on these inflammatory responses. Due to limited quantities of RA synovial fluids that we could obtain from a given patient, we first developed an understanding of the effects of recombinant cytokine stimuli and kinase-targeted drugs on

inflammatory responses of SFs, and then conducted a series of focused studies using synovial fluids from RA patients. We found that RA synovial fluids potently activated multiple stress-activated and inflammatory signaling pathways in SFs, such as the JNK, p38, and JAK/STAT pathways (see Table S1 for a list of abbreviations). Interestingly, this response was consistent across SF from healthy and RA tissues, suggesting that both normal and RA SFs are similarly capable of activation by inflammatory factors in the RA microenvironment. We also found that drugs targeting p38 significantly increased activation of pathways linked to RA progression specifically in the presence of inflammatory factors such as TNF α and IL-1 α , but not for the mitogenic stimulus EGF. To identify such context-dependencies from our large-scale data it was necessary to control for the confounding effects of multiple simultaneous perturbations (such as combinations of stimulatory cytokines and kinase-targeted inhibitors) by incorporating information about the experimental design into our statistical modeling analyses. Together, our findings characterize pathways activated in SFs by the inflamed synovial environment, provide evidence that negative regulatory cross-talk by p38 limited the clinical benefit of targeting p38 for RA, and demonstrate the utility of a broad perturbational framework for providing insight into multivariate drug effects.

Results

Characterization of signaling pathways activated in RA SF

SFs from RA patients display uniquely aggressive properties that are not observed in cells from normal or OA donors (14, 15). To characterize pathways activated in RA we measured the effects of disease-related inflammatory stimuli on intracellular signaling pathways believed to be involved in inflammatory cytokine signaling or SF biology (7, 26, 27) (Fig. 1A). Given their strong connection to RA the stimuli included TNF α , IL-1 α , and IL-6 (28, 29). We additionally included EGF as a stimulus due to its presence at high levels in the RA synovium (30) and as a positive control for activation of PI3K/AKT and MEK/ERK pathways, two canonical pathways of the EGF receptor. To compare potential differences in responsiveness between normal and RA SFs, we evaluated responses of SFs from four healthy and four RA human tissues. The primary human SFs were propagated in culture and then individually exposed to the stimuli for 10 or 30 min. Cells were then fixed and immunostained to measure phosphorylation or nuclear localization of the intracellular signaling nodes using high-throughput immunofluorescent microscopy and image analysis (Fig. S1 and Table S2). Cells were exposed to stimuli in biological quadruplicate (biological duplicates within experiments conducted on two separate days) to result in a compendium of ~5,000 data points quantifying the immediate-early signaling responses across multiple normal and RA SF samples (Fig. S2; SF sample information is in Table S3). Correlation of experimental replicates was generally high and consistent across SF samples and signaling nodes, indicating a high-quality dataset (average Pearson corr. = 0.75 across experimental replicates for 11/13 nodes; Fig. S3). An exception to this was p-JNK, whose correlation between the two experiments varied across the SF samples (correlation ranged from 0.51 to 0.86, $\rho_{\text{avg}} = 0.69$; Fig. S3). This may have been due to moderate anti-p-JNK antibody quality since p-c-Jun, a transcription factor downstream of JNK, was tightly correlated across experiments for all SF samples ($\rho = 0.97 \pm 0.02$). The other exception was p-AKT ($\rho =$

0.55±0.2). It's poor correlation across experiments appeared to result from activation of AKT primarily only by EGF in this dataset. This activation was additionally highly transient, peaking at 10 min and returning near to baseline levels by 30 min (Fig S2). Notably, these dynamics differ both from that of ERK activation, which was increased at both 10 and 30 min post-EGF stimulation (Fig. S2), and from AKT signaling in cancer cells lines exposed to EGF, which generally exhibit more sustained AKT activation through 90 min (31). Overall, we conclude this is a high-quality dataset for exploring SF activation in response to factors associated with RA.

To score pathways activated by each stimuli we analyzed the data using multiple linear regression (MLR; Figs. S4 and S5; see also the *Materials and Methods*), a useful method for determining input-output relationships between perturbations and cellular responses (32). This resulted in MLR models for each SF donor sample and time point in which the MLR β coefficients represented a model of the effects of each stimulus on a given signaling node. More sophisticated analyses are possible, but previous studies have shown that MLR performs well for data such as ours (32, 33), and we found MLR to be an interpretable and statistically rigorous approach to score pathway activities across multiple donor samples and stimuli. The MLR β coefficients were consistent across donor samples, with 93.5% of inferred connections occurring in at least six of the eight SF donor samples. IL-6 was the only stimulus to consistently induce JAK/STAT pathway activity across multiple SF donor samples (Fig. 1B and Fig. S5). TNF α , IL-1 α , and EGF each activated the mitogen-activated protein kinase (MAPK) pathways MEK, p38, and JNK, while TNF α and IL-1 α additionally activated the NF κ B pathway (Fig. 1B, Benjamini-Hochberg (34) false discovery rate (q_{BH}) < 0.01). The p38 and JNK pathways are key "stress" pathways involved in responses to stress stimuli, including inflammatory cytokines. Consistent with this function we found that activation of p38 and JNK signaling by EGF was much lower than that for TNF α or IL-1 α (Fig. S6). Notably, however, whereas activation of the MEK/ERK pathway, which is involved in cell proliferation and cell cycle progression, is usually low or absent for inflammatory stimuli as compared to mitogenic factors such as EGF (35), we found that maximal activation of the MEK/ERK pathway by TNF α and IL-1 α approached similar levels to that of EGF (Fig. S6).

To more broadly explore correlations among the measured signaling nodes we visualized the β coefficients for each cytokine and SF sample in a reduced dimensional space using principal component analysis (PCA). The resulting PCA coefficients reflect the covariance of the measured signaling nodes across stimuli, time points, and SF samples and are consistent with our understanding of kinase signaling network architecture. For example, projections of components within the same canonical pathway are largely aligned (namely, JNK pathway: p-JNK and p-c-Jun; p38 pathway: p-p38, p-Hsp27, and p-MK2; and JAK/STAT pathway: p-STAT1 and p-STAT3); and the projection of FoxO3a is approximately anti-parallel to p-AKT and p-ERK, which is consistent with the negative regulation of FoxO3a by the PI3K/AKT and MEK/ERK pathways (Fig. 1C). For a given time point, the projection of p-CREB is largely orthogonal to that of p-ERK and p-p38 (Fig. 1C). This would typically suggest independence from the MEK/ERK and p38 pathways, but a closer inspection suggests a more complicated interpretation. The strong activation of p-ERK by EGF at both 10 and 30 min post-stimulation results in the p-ERK coefficients projecting

towards the EGF scores (compare in Fig. 1C and 1D), while the strong activation of the p38 pathway by IL-1 α and TNF α results in the p-p38 coefficients projecting towards the IL-1 α and TNF α scores (compare in Fig. 1C and 1D). CREB is regulated by the MEK and p38 pathways (Fig. 1A) and is also activated by EGF, TNF α , and IL-1 α (Fig. 1B), which manifests as the p-CREB coefficients bisecting the p-ERK and p-p38 coefficients. Notably, the PCA scores of the MLR coefficients cluster according to stimulatory context, with no clear divergence between normal and RA SFs (Fig. 1D). Among individual stimuli the eight SF samples also displayed consistent activation and dynamics between both normal and RA SFs (Fig. S6). We conclude that the MLR networks (and the primary data from which they are derived) capture complex features of kinase signaling network architecture, which supports the utility of our perturbational approach for examining SF activation. In addition, for the stimuli examined here, stimulatory context plays a greater role in determining SF activation state than inherent differences between SF from normal and RA tissues.

Evaluation of multipathway effects of MAPK inhibitors

Inhibition of MEK, JNK, and p38 signaling has been explored previously for RA therapy (7, 23, 25). Although we found above that each of these pathways are strongly activated by TNF α and IL-1 α in SF, clinical studies of drugs targeting these pathways have resulted in limited benefit. To explore whether potential signaling pathway cross-talk might limit the benefit of inhibitors targeting these pathways, we evaluated the multivariate effects of drugs targeting MAPK signaling in SFs. We first explored the effects of two specific p38 inhibitors (SB202190 (36) and PH-797804 (37)) on p38 and JNK signaling. Both p38 inhibitors reduced p38 pathway activity (as monitored by p-Hsp27), but also elevated JNK pathway activity in a dose-dependent manner (as monitored by p-c-Jun) specifically at a late time point (90 min post-stimulation) but not at an early/intermediate time point (30 min post-stimulation, Fig. 2, A–C). To systematize this analysis, we needed to incorporate context into our analytical framework. For example, in considering the opposite effects of the p38 inhibitor SB202190 on p-Hsp27 and p-c-Jun at the 90-min time point (Fig. 2B), one might expect that the data for these two signaling nodes are negatively correlated. Such a correlation, however, does not reach a level of statistical significance (Fig. 2D, $p=0.087$) due to the confounding effect of IL-1 α , which activates both nodes. As shown above, we can control for the effect of IL-1 α on these signaling nodes using MLR by regressing the data for each signal against the presence or absence of IL-1 α . The unexplained effect of each signal (that is, the MLR model residuals) should contain information about the inhibitor, which represents an experimental perturbation that was deliberately unaccounted for in the model. Removal of the IL-1 α dependency in this manner highlights the significant negative correlation between p-Hsp27 and p-c-Jun ($p=2.1\times 10^{-6}$, Fig. 2E). This analysis is referred to as partial correlation (38) because it analyzes the correlation between two variables (in this case, p-Hsp27 and p-c-Jun) that is not explained by a third variable (IL-1 α stimulation). Applying this partial correlation analysis framework to the full dataset (Fig. 2, A and B) revealed that this negative partial correlation is consistent for both p38 inhibitors (partial corr. at 90 min = -0.8 to -0.9 and $p<0.0001$), a relationship that is not detectable by traditional correlation analysis (Fig. 2, F and G). Thus, when evaluating relationships from multi-perturbation experiments (stimulus and inhibitor combinations, for example), explicitly including aspects of the experimental design in the analytical framework can help

control for effects of individual perturbations and uncover significant associations in the data.

To explore multipathway effects of inhibitors against each of the three MAPK pathways we measured the effects of specific p38 (PH-797804), JNK (JNK-IN-8) (39), or MEK (PD184352) (36, 40) inhibitors on signaling in SFs after 90 min incubation with IL-1 α (Fig. 3A; additional inhibitor information in Table S4). We selected phosphorylation of c-Jun, Hsp27, and ERK, which are downstream nodes of JNK, p38, and MEK, respectively, as activity readouts for these pathways (Fig. 3A). We performed independent experimental replicates on separate days (Fig. 3B), and then analyzed each experimental replicate using partial correlation as described above (Fig. 3C). We then merged the p-values from the independent experimental replicates using a modified Fisher method (41, 42). This analysis reproduced the negative partial correlation between the p38 and JNK pathways in the presence of p38 inhibition (Fig. 3D, partial corr.= -0.72 , $q_{BH}<10^{-8}$). The increased significance observed here compared to above results from the increased statistical power by merging inferences across experimental replicates using Fisher's method. This analysis additionally revealed a significant negative partial correlation between the p38 and MEK pathway (Fig. 3D, partial corr.= -0.80 , $q_{BH}<10^{-10}$), demonstrating increased activation of both the MEK and JNK pathways by p38 inhibition. The positive partial correlation between p-CREB and p-Hsp27 (Fig. 3D) is the result of at least partial regulation of these nodes by p38 in SFs. This positive partial correlation for p38 inhibition coupled with the lack of a positive partial correlation between p-CREB and p-ERK for MEK inhibition (Fig. 3D) suggests that, although CREB is activated by both the p38 and MEK/ERK pathways (Fig. 1), CREB activity is primarily driven by the p38 pathway in SFs activated with IL-1 α . The JNK inhibitor and the MEK inhibitor each enhanced p38 pathway activity; however, this effect was weaker than the converse effect of increased JNK and MEK pathway activity by p38 inhibition discussed above (Fig. 3, D and E). We did not detect crosstalk between JNK and MEK (Fig 3D), despite such crosstalk being reported in other cell types (43–45). A traditional correlational analysis that does not control for the effect of IL-1 α is dominated by the positive effect of IL-1 α on MAPK signaling, and fails to accurately characterize the presence or absence of multivariate inhibitor effects for the MEK, JNK, or p38 inhibitors (Fig. S7). Overall, we conclude that the p38 pathway exhibits greater multi-pathway control in SF than the other MAPK pathways MEK and JNK, and that inhibition of p38 results in significantly elevated MEK and JNK signaling due to relief of this negative regulatory cross-talk.

Context dependence of pathway cross-talk

To further explore the relationship between stimulatory context and multipathway effects of p38 inhibition, we examined SF signaling responses on the background of the diverse signaling network states induced by IL-1 α , TNF α , EGF, or IL-6. Following 90 min stimulation in the presence or absence of the p38 inhibitor PH-797804 we measured the activation of 10 signaling proteins and transcription factors within the NF κ B, p38, MEK/ERK, PI3K/AKT, JNK, or JAK/STAT pathways using high-throughput microscopy (schematically depicted in Fig. S8A). The experiment was repeated in the same SF donor sample on separate days, with one experimental replicate comprising titration of the p38

inhibitor in biological duplicate and the second experimental replicate comprising at least four biological replicates with the p38 inhibitor at a concentration above its IC₉₀ (0.6 μM; Fig. S8, B and C). We performed the partial correlation analysis as described above to evaluate the correlation between the effects of the p38 inhibitor on the p38 pathway (through p-Hsp27) and the alternative pathways when controlling for the primary effects of each individual stimulus. The two experimental replicates were analyzed separately and p-values were merged using the modified Fisher method (41). We found that inhibiting the p38 pathway increased MEK, JNK, and NFκB signaling within the context of IL-1α and TNFα stimulation (as evidenced by their negative partial correlation to p-Hsp27 for these stimuli in Fig. 4A). In the context of EGF stimulation, however, only JNK signaling was increased by p38 inhibition (Fig. 4A). To further examine crosstalk by p38 we evaluated additional p38 inhibitors, including four that were tested in Phase II clinical trials for RA. The increased activation of IL-1α- and TNFα-induced NFκB, JNK, and MEK pathways was consistent across all six p38 inhibitors (Fig. 4B). It was also consistent across TNFα and IL-1α concentrations ranging from 0.1 – 100 ng/mL (Fig. 4C), suggesting such effects would be relevant in the face of variations of TNFα or IL-1α across patients or disease status. Together, this demonstrates that the p38 inhibition elevates the activities of multiple alternative pathways, and these multipathway effects are most pronounced for inflammatory stimuli such as TNFα or IL-1α.

Notably, the enhancement of MEK signaling by p38 inhibition does not appear to propagate downstream to CREB (Fig. 4A). To explore this in more detail, we reanalyzed the data for MEK and p38 inhibition (from Fig. 3). We did not observe a significant pairwise correlation between MEK pathway activity (via p-ERK) and p-CREB (Fig. 4D, p=0.66). However, controlling for the positive correlation between p-CREB and p38 pathway activity (through p-Hsp27; Fig. 4E) identifies a significant positive relationship between MEK signaling and p-CREB (Fig. 4F, p=2.2×10⁻⁶). This suggests that the increased MEK/ERK signaling is indeed propagated downstream to CREB, despite CREB activity in response to IL-1α stimulation being dominated by the p38 pathway. Moreover, these findings demonstrate the strength of combining broad perturbational experiments with multivariate analyses to identify network connections in the face of multiple confounding factors.

CREB as a key regulator of context-dependent cross-talk

To further evaluate the relationship between stimulatory context and multipathway effects of p38 inhibitors, as well as the relative absence of such effects for JNK and MEK inhibitors, we explored potential mechanisms of cross-talk by the p38, JNK, and MEK/ERK pathways. One method of cross-talk involves the regulation of phosphatases that act on neighboring pathways. The p38 and MEK/ERK pathways (through CREB) and JNK (through c-Jun) can each activate dual specificity protein phosphatase 1 (DUSP1, also called MAP kinase phosphatase 1, or MKP-1), which provides negative feedback regulation to the p38 and JNK pathways (25, 46–49) (Fig. 5A). A relatively specific inhibitor of DUSP1 (50) strongly elevated both p38 and JNK pathway activities (Fig. 5B). Additionally, SB747651A, which is a specific inhibitor of mitogen- and stress-activated protein kinases 1 and 2 (MSK1/2) and ribosomal S6 kinases 1 and 2 (RSK1/2), two structurally homologous upstream regulators of CREB (51, 52), increased p38 and JNK signaling in SFs (Fig. 5B). Combination of

SB747651A with p38 inhibition, however, did not further augment IL-1 α -induced JNK signaling relative to p38 inhibition alone (Figure 5C). Together, these observations suggest that feedback regulation by DUSP1 at least partially mediates the p38-dependent pathway cross-talk that we observe in SFs. These data also underscore a role for CREB in feedback regulation by p38 and are consistent with our observations above suggesting p38 signaling plays a dominant role in CREB signaling in activated SFs.

The question remains, however: if phosphatases that are regulated by JNK, p38, and ERK pathways mediate pathway cross-talk in SF, why do p38 inhibitors show dominant multipathway effects in SF while JNK and MEK inhibitors are much more modest? We reasoned that context-dependent regulation of CREB signaling may play a role in the differential multipathway effects. To further explore this context-dependence we reanalyzed the SF network activation data (from Fig. 1) by averaging the MLR β coefficients across time and RA SF sample and plotting as a node-edge graph in which the width of the edge is proportional to the strength of the averaged β coefficients (Fig. 6A). Though many of the same pathways are activated by the inflammatory stimuli IL-1 α and TNF α , and the mitogenic stimulus EGF, these stimuli differ strongly in their magnitude of activation: IL-1 α and TNF α more strongly activate the NF κ B, JNK, and p38 pathways, while EGF more strongly activates the MEK/ERK pathway (Fig. 6A). We further reanalyzed the kinetics of p38 and MEK activation by TNF α , IL-1 α , and EGF and found that while these stimuli induced different dynamics for MEK/ERK and p38 signaling, they nevertheless converged to consistent signaling at the level of CREB (Fig 6B). We conclude that CREB acts as an integrator of p38 and MEK/ERK pathway activities and its activation is dominated by p38 signaling in response to TNF α and IL-1 α , but by MEK/ERK signaling in response to EGF.

To explore a role for CREB in context-dependent crosstalk in SFs, we evaluated the multipathway effects of MEK and p38 inhibitors under mitogenic and inflammatory contexts. Strikingly, whereas MEK inhibition minimally affected p38 pathway activity within the context of IL-1 α stimulation (Fig. 3), it strongly increased EGF-induced p38 activity (as assayed by p-Hsp27) (Fig. 6C). These relationships are reversed from that of the p38 pathway: p38 inhibition minimal affected EGF-induced MEK/ERK pathway activity (Fig. 6B), in contrast to its strong enhancement of IL-1 α - or TNF α -induced MEK/ERK activity (Fig. 4, A–C). The more limited multipathway effects of p38 inhibition for EGF stimulation as compared to IL-1 α or TNF α stimulation was consistent across four normal and four RA SF samples (Fig. 6D and Fig. S9) and across dermal fibroblast and mammary epithelial cell lines (Fig. 6E), suggesting that the context-dependence characterized in this study is a general feature of p38 signaling. Overall, these data reveal a critical role for CREB signaling in context-dependent multipathway crosstalk by the MEK/ERK or p38 pathways and demonstrate how stimulatory environment influences which pathways dominate crosstalk even within a fixed signaling network topology (Fig. 6F). This in turn results in marked differences for the effects of drugs targeting MEK or p38 depending on whether the context is inflammatory or mitogenic.

Decoupling pathway cross-talk and pathway inhibition

To assess whether inhibiting additional pathways could decouple the multipathway effects of p38 inhibition, we evaluated combinations of JNK or MEK inhibitors with p38 inhibition. Titration of the JNK inhibitor JNK-IN-8 in the presence of IL-1 α and the p38 inhibitor PH-797804 blocked the enhanced activation of the JNK pathway in a dose-dependent manner as expected, but did not mitigate that of NF κ B or MEK signaling by the p38 inhibitor (Fig. S10A). Similarly, titration of the MEK inhibitor PD325901 in the presence of IL-1 α and PH-797804 specifically blocked crosstalk to the MEK pathway. This combination did, however, result in further enhancement of NF κ B nuclear translocation beyond that of p38 inhibition alone (Fig. S10B). Notably, MEK inhibition in the absence of the p38 inhibitor did not affect NF κ B nuclear translocation (Fig. S10C), suggesting coordinate downregulation of NF κ B signaling by p38 and MEK signaling.

We further evaluated whether inhibitors against nodes upstream or downstream of p38 could also decouple the desirable inhibition from the pathway crosstalk. Transforming growth factor- β -activated kinase 1 (TAK1, also known as MAP3K7) lies upstream of p38, JNK and NF κ B signaling (Fig. 5A) and regulates much of the inflammatory cytokine secretion by activated SF in RA (12). The TAK1 inhibitor (5z)-7-oxozeaenol (5ZO) inhibited both the primary activation of NF κ B, JNK, p38, and MEK/ERK signaling induced by TNF α and IL-1 α (Fig. S11A) and blocked the increased signaling conferred by p38 inhibition (Fig. S11B). Known polypharmacology of 5ZO towards MEK1/2 (International Centre for Kinase Profiling, <http://www.kinase-screen.mrc.ac.uk/kinase-inhibitors>) likely contributes to the inhibition of ERK activation that we observe here. MAPK-activated protein kinase-2 (MAPKAP-2 or MK-2) lies downstream of p38 and promotes inflammatory cytokine production (23). In contrast to direct p38 inhibition, MK-2 inhibition did not exhibit multipathway effects (Fig. S11C). We conclude that combinations of MAPK inhibitors or inhibition of nodes upstream or downstream of p38 can decouple multipathway crosstalk to result in more effective suppression of inflammatory signaling in SFs.

Activation of SFs by RA synovial fluids

Based on the understanding of the SF signaling network developed above, we examined pathways activated in SFs by the disease-relevant context of RA synovial fluids. SFs from one RA donor were exposed to serially diluted RA synovial fluids, and signaling activation was measured using high-throughput immunofluorescent microscopy. Due to limited quantities of RA synovial fluids we pooled equal volumes of fluids from two RA patients and diluted them in basal SF medium (Pooled RA Fluids_{CD}; information on synovial fluids is in Table S5). Synovial fluid naturally functions as a joint lubricant and is present in only very small amounts in healthy patients; synovial fluids from healthy individuals were thus not available for comparison due to challenges in collecting such material (53). The pooled RA synovial fluids significantly activated the JNK, MEK, and p38 pathways (through p-c-Jun, p-ERK, and p-Hsp27, respectively; Student's t-test $p < 10^{-9}$) and reached similar levels of activation as saturating doses of TNF α (Fig. 7A). Up to 64-fold dilution of the pooled RA synovial fluids continued stimulating activation of these pathways to at least two-fold above unstimulated levels (Fig. 7A). The RA synovial fluids also significantly activated p-STAT1 ($p < 10^{-14}$), with up to 16-fold dilution of the pooled RA fluids resulting in p-STAT1

activation to at least two-fold above the assay background (Fig. 7A). We detected statistically significant nuclear translocation of NF κ B ($p < 10^{-8}$), but the effect size was smaller than activation of MAPK or JAK/STAT signaling (Fig. 7A). Individual evaluation of RA synovial fluids from three separate patients resulted in nuclear translocation of NF κ B (up to 1.5 fold assay background) in one of the RA synovial fluid samples and increased activation of p-STAT3 by the same sample, suggesting that RA synovial fluids from different donors can variably activate SF signaling (Fig. 7B). Moreover, this demonstrates that RA synovial fluids can activate both pro-inflammatory (STAT1, Fig. 7A) and anti-apoptotic, pro-proliferative (STAT3, Fig 7B) branches of the JAK/STAT pathway in SFs (54), which would support both the pro-inflammatory and hyperplasia phenotypes of activated SFs in RA. The pathways activated by RA synovial fluids were consistent across SFs from two normal and two RA donors (Fig. 7C and Fig. S12A). Notably, pooled OA synovial fluids exhibited similar activity to RA synovial fluids on both normal and RA SFs (Fig. 7C and Fig. S12A). We conclude that inflammatory factors in RA and OA synovial fluids strongly activate intracellular kinase signaling in SFs, and this signaling response is consistent across SFs from normal and RA donors.

Because synovial fluids activate many of the pathways that are regulated by TAK1 in activated SFs or increased by p38 inhibitors in inflammatory contexts, we investigated the effects of p38 or TAK1 inhibition on the activation of SFs by RA synovial fluid. Due to limited quantities of RA synovial fluids we examined a single concentration of the p38 inhibitor (PH-797804 at 0.6 μ M) in biological duplicate (Fig. S12B). Inhibition of p38 increased the activity of both MEK and JNK pathways induced by the RA synovial fluids, consistent with our previous observations for stimulation with IL-1 α or TNF α (Fig. 7D, partial corr. = -0.77 and -0.79, $q_{BH} < 0.1$). For 5ZO, we compared its effects with the FDA-approved JAK inhibitor tofacitinib. Whereas tofacitinib inhibited only JAK/STAT signaling, 5ZO significantly inhibited activation of the JNK, p38, and MEK/ERK pathways induced by RA synovial fluids and not the JAK/STAT pathway (Fig. 7E). Together, this demonstrates that p38 inhibition elicits compensatory signaling responses within the within the complex environment of RA synovial fluids. By comparison, 5ZO is capable of normalizing SF activation in a manner that is complementary to existing treatment options for RA.

Discussion

In this study, we used a systematic approach to analyze the multivariate effects of kinase inhibitors on inflammatory signaling responses. The effects of the inhibitors were complex and challenged traditional approaches for evaluating intracellular signaling. We therefore applied an analytical framework that controlled for multiple confounding factors while identifying statistically significant associations within the data. We found that p38 functioned as a uniquely central node that regulated the activity of multiple other pathways specifically in inflammatory, but not mitogenic, contexts, and its inhibition strongly elevated NF κ B, JNK, and MEK/ERK activity. Such an effect is clinically undesirable given the connections of these pathways to inflammation and RA progression (7, 55, 56) and likely played a role limiting the clinical benefit of p38 inhibitors for RA.

A characteristic feature of RA is a self-sustaining inflammatory microenvironment in affected joints. Our findings suggest that SFs function in a positive feedback loop to help sustain this microenvironment. RA synovial fluids provoked a strong inflammatory signaling response in *ex vivo* cultures of SFs and induced the activation of the p38, JNK, and MEK pathways to similar levels as saturating amounts of TNF α . Whereas RA SFs display a uniquely aggressive phenotype (7, 9), we observed similar activation of both normal and RA SFs by RA synovial fluids. These findings suggest that soluble factors from the RA microenvironment prime the resident SFs towards the aggressive, activated phenotype observed in RA. We have previously reported that cytokines secreted by *ex vivo* cultures of activated SFs are enriched in the synovial fluids of RA patients (12). Activated SFs are also capable of presenting arthritogenic peptides to T cells, further promoting RA pathogenesis (57). Taken together, these observations support a complex relationship between SFs and their environment in RA, in which SFs are directly activated by the inflamed RA microenvironment and activated SFs further perpetuate this inflammation and autoimmunity.

Intracellular signaling pathways are highly interconnected, and in this study we found a critical role for stimulatory context in determining which signaling pathway dominates negative regulatory crosstalk. Such a context-dependence resulted in dramatic differences in drug effects depending on stimulatory context and has strong implications for understanding how successful versus unsuccessful therapeutic interventions may be biologically conditioned. For example, we found contrasting effects of drugs targeting p38 or MEK depending on whether the context was primarily inflammatory or mitogenic: p38 inhibitors exhibited greater multipathway effects in pro-inflammatory environments, while multipathway effects of MEK inhibition were more prominent for mitogenic than inflammatory contexts.

CREB emerged as a key nexus for these context-dependent inhibitor effects. It is activated by both the MEK and p38 pathways, and upon activation it regulates expression of phosphatases that downregulate MAPK activity (48, 49). CREB thus functions in part within a negative regulatory feedback loop for MAPK signaling. We found that stimulatory context strongly influenced the regulation of CREB by the MEK or p38 pathways: for the inflammatory stimuli TNF α and IL-1 α CREB activity is dominated by the p38 pathway, while for the mitogenic stimulus EGF CREB activity is dominated by the MEK/ERK pathway. We reason that feedback via a MEK/CREB axis is suppressed in inflammatory contexts due to the dominance of p38 on CREB activity. For mitogenic contexts the converse is true: the dominance of MEK signaling on CREB activity suppresses potential negative regulatory feedback from a p38/CREB axis. The p38 pathway can provide additional negative regulatory feedback through its activation of protein phosphatase 2A (PP2A), which negatively regulates JNK and MEK/ERK activity (58, 59), and through negative regulatory feedback to TAK1, an upstream regulator of p38, JNK, and NF κ B signaling (60, 61) (Fig. 5A). For stimulatory contexts that strongly activate p38, these additional mechanisms of crosstalk would further strengthen the role of p38 in downregulating activated intracellular signaling.

Although p38 inhibition is no longer under clinical investigation for RA, it has generated interest for a range of disorders involving dysregulated inflammation such as multiple

sclerosis (62), chronic obstructive pulmonary disorder (COPD) (63), atherosclerosis (64, 65), diabetic cardiomyopathy (66), and neuropathic pain (67, 68). Our findings argue for careful analysis of the effects of p38 inhibitors on multiple potential compensatory pathways and on the background of multiple disease-relevant contexts to understand the full effects of drugs targeting p38 in inflammation-related disorders. We found that cross-talk by p38 could be decoupled through combinations of inhibitors or by targeting nodes upstream or downstream of p38, such as TAK1 or MK2. This suggests alternative therapeutic strategies can maintain at least part of the benefits of direct p38 inhibition, while limiting the undesirable effects of relieving negative regulatory cross-talk by p38. More broadly, our work suggests a more systematic analysis of potential multipathway effects of drug-candidates should be included as part of a clinical development program. Such experimentation and analysis can help clarify the risks of developing drugs targeting nodes believed to be involved in multipathway crosstalk.

Materials and Methods

Antibodies and reagents

Tumor necrosis factor- α (TNF α ; cat. no. 300-01A), interleukin-1 α (IL-1 α ; cat. no. 200-01A), interleukin-6 (IL-6; cat. no. 200-06), and epidermal growth factor (EGF; cat. no. AF-100-15) were purchased from PeproTech. Chemical inhibitors from the following sources were dissolved in dimethyl sulfoxide (DMSO) to 10 mM stock concentrations: TAK1 inhibitor (5z)-7-oxozeaenol (cat. no. 3604), p38 inhibitor EO 1428 (cat. no. 2908), MSK/RSK inhibitor SB747651A (cat. no. 4630), and PP2A inhibitor okadaic acid (cat. no. 1136) were purchased from Tocris Bioscience; P38 inhibitors PH-797804 (cat. no. S2726), SB202190 (cat. no. S1077), VX-702 (cat. no. S6005), BIRB 796 (cat. no. S1574), and LY2228820 (cat. no. S1494), MEK inhibitor PD184352 (also referred to as CI-1040; cat. no. S1020), and JAK inhibitor tofacitinib (also referred to as CP-690550; cat. no. S2789) were purchased from Selleck Chemicals; DUSP1/6 inhibitor BCI was purchased from Axon Medchem (cat. no. 2178); MK-2 inhibitor III (cat. no. 475864) and inhibitor IV (cat. no. 475964) were purchased from EMD Millipore; JNK inhibitor JNK-IN-8 was kindly provided by the Nathanael Gray Lab, Dana Farber Cancer Institute. Phospho-p44/42 MAPK (ERK1/2)^{T202/Y204} (cat. no. 4370), phospho-Hsp27^{S82} (cat. no. 9709), phospho-c-Jun^{S73} (cat. no. 3270), phospho-STAT1^{Y701} (cat. no. 9167), phospho-STAT3^{Y705} (cat. no. 9145), phospho-S6^{S235/236} (cat. no. 4858), phospho-CREB^{S133} (cat. no. 9198), phospho-AKT^{S473} (cat. no. 4060), phospho-MK2^{T334} (cat. no. 3007), phospho-JNK^{T183/Y185} (cat. no. 9251), phospho-p38^{T180/Y182} (cat. no. 4511), FoxO3a (cat. no. 2497), NF κ B p65 (cat. no. 8242) were purchased from Cell Signaling Technology; NF κ B p65 (cat. no. sc-8008) was purchased from Santa Cruz Biotechnology. Fluorescently labeled secondary antibodies donkey anti-mouse IgG polyclonal antibody (pAb) 488 conjugate (cat. no. A21202) and donkey anti-rabbit IgG pAb Alexa 647 Alexa conjugate (cat. no. A31573) were purchased from ThermoFisher Scientific. RA synovial fluids were purchased from Analytical Biological Services, Inc and kindly provided by J. Swantek at Boehringer Ingelheim, Inc. (see Table S5 for details).

Tissue culture

Normal primary human synovial fibroblasts (SF; human fibroblast-like synoviocytes, HFLS, cat. no. 408-05a) and RA SF (HFLS-RA, cat. no. 408RA-05a) were purchased from Cell Applications, Inc (see Table S3 for details). The nomenclature used for SF samples denotes lot number (e.g. N2586 is Cell Applications HFLS lot no. 2586, RA2159 is Cell Applications HFLS-RA lot no. 2159, etc). Cells were cultured according to the supplier's recommendations using Synoviocyte Growth Medium (Cell Applications, Inc. cat. no. 415-500); Synoviocyte Basal Medium (Cell Applications, Inc. cat. no. 414-500) was used for serum starvation prior to experimental treatments. Cells were provided at passage 2 and all experiments were conducted at passage 3 – 6, in line with published recommendations (69).

Signaling response seeding and treatments

Signaling responses of cultured SF were examined as previously described (12). Briefly, SF were seeded (600 cells/well) into 384-well plates; following ~24 incubation in full growth medium cells were starved in basal medium overnight (~16 hr) followed by a refresh of basal medium approximately 4 hr prior to exposure to stimulatory factors. For experiments involving inhibitors, cells were pretreated with inhibitor or DMSO control for ~2.5 hr prior to stimulation with 100 ng/mL TNF α , IL-1 α , IL-6, or EGF (diluted into basal SF medium containing 0.1% bovine serum albumin, BSA) at a final volume of 50 μ L/well; DMSO was maintained at a constant concentration for all experimental treatments (e.g. for experiments with a maximum inhibitor concentration of 3 μ M, DMSO was maintained at a 1:3333 dilution for all treatments in the experiment, which corresponds to the amount of DMSO in 3 μ M of inhibitor diluted from a 10 mM stock concentration). To support reproducibility, all inhibitor and stimulus treatments were performed using automated liquid handling instruments (Biomek FX by Beckman Coulter or ID STARlet by Hamilton) at the Harvard Medical School Longwood Screening Facility.

Immunofluorescent microscopy and analysis

Measurement of signaling intensity by immunofluorescent microscopy was conducted as previously described (12). Briefly, cells were fixed in 2% paraformaldehyde for 10 min, washed 3 \times for 5 min in 1 \times PBS with 0.1% Tween-20 (PBST), permeabilized with 100% methanol for 10 min, washed 3 \times with PBST, and blocked with Odyssey Blocking Buffer (OBB; LI-COR) for 1 hr. Cells were stained overnight at 4 $^{\circ}$ C with 25 μ L of primary antibodies diluted in OBB (see Table S2 for dilution ratios for each antibody). Cells were washed 3 \times with PBST and stained with 25 μ L appropriate secondary antibodies diluted 1:2000 in OBB and incubated 1 hr. Cells were washed 1 \times in PBST, 1 \times in PBS, and incubated with Hoechst-33342 (0.25 μ g/mL; Invitrogen cat. no. H3570) and Whole Cell Stain Green or Blue (1:1000 dilution; Thermo Fisher cat. nos. 8403202 and 8403502) in PBS for 30 min. Cells were washed 2 \times in PBS and imaged using a 10 \times objective on an Operetta high-throughput microscope using Harmony software (PerkinElmer, Inc.).

Data were extracted from images using Columbus software (PerkinElmer, Inc.). Briefly, Hoechst-33342 and Whole Cell Stain Green (or Whole Cell Stain Blue) signals were used to segment the nuclear and cellular boundaries. These segmented boundaries were then used to

define nuclear, cytoplasmic, and whole cell “regions” that were more narrowly defined than the segmented boundaries in order to accommodate potential errors by automated segmentation (see Fig. S1). We defined ‘ring regions’ for each cell to control for fluctuations in the local background (due to dust, bubbles, or non-flat illumination, for example). The ring regions comprised the 5–12 pixels beyond the cellular segmented boundary that was devoid of neighboring segmented cells. Cell-specific local background intensity was quantified from the individual ring regions and used to normalize signals for nuclear, cytoplasmic, and whole cell regions. To quantify NFκB nuclear translocation nuclear/cytoplasmic ratios were calculated for each cell. For other signals, single-cell intensities were extracted for the appropriate cellular region; for example nuclear intensity was used for phosphorylated transcription factors such as p-c-Jun, p-STAT1, and p-STAT3, while whole cell or cytoplasmic intensity was used for p-ERK1/2 and p-HSP27 (see Table S2 for cellular region for each measured signaling protein). Median values of single-cell distributions within an individual well were used for all subsequent analyses.

MLR of signaling network responses

A multiple linear regression (MLR) framework of the form $y = X\beta + e$ was used to infer connections between stimuli and signaling network proteins from perturbational data. The predictor matrix X encodes an experimental design matrix, with the columns denoting the presence (1) or absence (0) of a given stimulus and the rows denoting individual experimental conditions; unstimulated background was denoted as a column of 1s. The response matrix y comprises the measured signal intensities for the experimental conditions (rows) across each measured signaling protein or transcription factor (columns). β is a vector of regression coefficients relating the effects of the stimuli in X to the signals in y ; and e is a vector of model residuals. We used MLR to solve for the β coefficients using the Matlab `regstats.m` function. This approach was employed for each donor sample, time point, and independent experimental replicate.

For a multivariate analysis of inhibitor effects, MLR beta coefficients for each signaling network protein were scaled to a maximum of 1 for the maximum value observed across all stimulatory contexts, SF samples, experimental replicates, and time points. Scaled MLR coefficients were then compiled across all conditions (4 stimuli \times 8 SF samples \times 2 experimental replicates = 64 rows) and all signaling network proteins and times points (13 signaling proteins \times 2 time points = 26 columns). The matrix of compiled MLR coefficients were mean centered (column-wise) and then analyzed by principal component analysis (PCA) using the Matlab `pca.m` function.

Consistency of network activation across donors

To evaluate consistency of network activation across SF samples we first merged the p-values of the independent experimental replicates for a given time point and SF sample using a modified Fisher method, which allows the use of two-sided p-values (41, 42). and controlled for the false-discovery rate (FDR) of the resulting merged p-values using the Benjamini-Hochberg method (34). To account for dynamics of a given signal, which may be active at one time point, but not another, a connection between a given stimulus and a given signal was taken to be present if the FDR-corrected, merged p-value was less than 0.01 at

either time point (10 or 30 min post-stimulation; see Fig. S3). The strength of a connection was determined by merging MLR coefficients across experimental replicates and time. The consistency of connections was summed across the eight SF samples (four normal and four RA SF).

Partial correlation

Partial correlation is useful for evaluating correlations between pairs of variables while controlling for the variance explained by a third variable. We employed this approach to evaluate correlations induced by specific pathway inhibitors using data from multi-perturbational experiments. Briefly, data was \log_{10} -transformed and basal signal (no stimulus and no inhibitor) was set to 0 for each signaling network protein, and then variance explained by stimuli was controlled using the MLR framework described above. The residuals of this model (ϵ) contain information about the effect of inhibitors. Data for a downstream signaling node was used as a handle for monitoring the effect of inhibitor titrations on pathway activities: p-Hsp27 was used as a handle for p38 pathway activity with the p38 inhibitor; p-c-Jun was used for JNK pathway activity with the JNK inhibitor; and p-ERK was used for MERK/ERK pathway activity with the MEK inhibitor. The residuals for each stimulus and inhibitor context were partitioned along with a randomly selected subset of the control replicates (i.e. basal levels and stimulus in the absence of inhibitor) in order to avoid repeated use of control samples. Finally, for each stimulus and inhibitor context we calculated the correlation between residuals of the respective proximal pathway target and other signaling network proteins using the Matlab `corr.m` function. These correlations between residuals are the reported partial correlations. P-values for independent experimental replicates conducted on separate days were merged using a modified Fisher's method (41, 42), and false discovery rate from multiple hypothesis testing was controlled using the Benjamini-Hochberg method (34).

Statistical analysis of serial dilutions and tofacitinib and 5ZO effects

Data were \log_{10} -transformed to stabilize variance. Significance of stimulated response data in comparison to the unstimulated signal was evaluated using an unpaired two-sample Student's t-test with equal variance using the Matlab `ttest2.m` function. False discovery rate for the RA synovial fluid serial dilutions was controlled using the Benjamini-Hochberg-Yekutieli method for positive dependence (70). Significance of tofacitinib or 5ZO inhibitor effects in comparison to the uninhibited stimulated signal was evaluated using an unpaired two-sample Student's t-test with equal variance using the Matlab `ttest2.m` function.

Supplementary Material

Refer to Web version on PubMed Central for supplementary material.

Acknowledgments

We thank S. Rudnicki and the Harvard ICCB for assistance developing automated protocols for stimuli and inhibitor treatments; D. Clarke, M. Morris, and J. Copeland for helpful discussions; J. Swantek at Boehringer Ingelheim, Inc. for providing the synovial fluids; and N. Gray and T. Zhang at DFCI for providing JNK-IN-8.

Funding: This work was supported by the NIH LINCS grant U54HL127365, and P50 GM107618, a grant dated 8/1/2009 from Boehringer Ingelheim Inc., the Army Research Office Institute for Collaborative Biotechnologies grant W911NF-09-0001, and an NIH NRSA Fellowship 5F32AR062931 to D.S.J.

References and Notes

1. Scott DL, Wolfe F, Huizinga TW. Rheumatoid arthritis. *The Lancet*. 2010; 376:1094–1108.
2. McInnes IB, Schett G. The pathogenesis of rheumatoid arthritis. *N Engl J Med*. 2011; 365:2205–2219. [PubMed: 22150039]
3. Dadoun S, Zeboulon-Ktorza N, Combescure C, Elhai M, Rozenberg S, Gossec L, Fautrel B. Mortality in rheumatoid arthritis over the last fifty years: systematic review and meta-analysis. *Joint Bone Spine*. 2013; 80:29–33. [PubMed: 22459416]
4. Firestein GS. Evolving concepts of rheumatoid arthritis. *Nature*. 2003; 423:356–361. [PubMed: 12748655]
5. Fox DA. The role of T cells in the immunopathogenesis of rheumatoid arthritis: new perspectives. *Arthritis & Rheumatism*. 1997; 40:598–609. [PubMed: 9125240]
6. Neumann E, Lefèvre S, Zimmermann B, Gay S, Müller-Ladner U. Rheumatoid arthritis progression mediated by activated synovial fibroblasts. *Trends in Molecular Medicine*. 2010; 16:458–468. [PubMed: 20739221]
7. Bottini N, Firestein GS. Duality of fibroblast-like synoviocytes in RA: passive responders and imprinted aggressors. *Nat Rev Rheumatol*. 2013; 9:24–33. [PubMed: 23147896]
8. Kiener HP, Watts GFM, Cui Y, Wright J, Thornhill TS, Sköld M, Behar SM, Niederreiter B, Lu J, Cernadas M, Coyle AJ, Sims GP, Smolen J, Warman ML, Brenner MB, Lee DM. Synovial fibroblasts self-direct multicellular lining architecture and synthetic function in three-dimensional organ culture. *Arthritis & Rheumatism*. 2010; 62:742–752. [PubMed: 20131230]
9. Filer A. The fibroblast as a therapeutic target in rheumatoid arthritis. *Current Opinion in Pharmacology*. 2013; 13:413–419. [PubMed: 23562164]
10. Bartok B, Firestein GS. Fibroblast-like synoviocytes: key effector cells in rheumatoid arthritis. *Immunological Reviews*. 2009; 233:233–255.
11. Noss EH, Brenner MB. The role and therapeutic implications of fibroblast-like synoviocytes in inflammation and cartilage erosion in rheumatoid arthritis. *Immunological Reviews*. 2008; 223:252–270. [PubMed: 18613841]
12. Jones DS, Jenney AP, Swantek JL, Burke JM, Lauffenburger DA, Sorger PK. Profiling drugs for rheumatoid arthritis that inhibit synovial fibroblast activation. *Nature Chemical Biology*. 2017; 13:38–45. [PubMed: 27820799]
13. Müller-Ladner U, Kriegsmann J, Franklin BN, Matsumoto S, Geiler T, Gay RE, Gay S. Synovial fibroblasts of patients with rheumatoid arthritis attach to and invade normal human cartilage when engrafted into SCID mice. *Am J Pathol*. 1996; 149:1607–1615. [PubMed: 8909250]
14. Lefèvre S, Knedla A, Tennie C, Kampmann A, Wunrau C, Dinser R, Korb A, Schnäker EM, Tarner IH, Robbins PD, Evans CH, Stürz H, Steinmeyer J, Gay S, Schölmerich J, Pap T, Müller-Ladner U, Neumann E. Synovial fibroblasts spread rheumatoid arthritis to unaffected joints. *Nature Medicine*. 2009; 15:1414–1420.
15. Pap T, Aupperle KR, Gay S, Firestein GS, Gay RE. Invasiveness of synovial fibroblasts is regulated by p53 in the SCID mouse in vivo model of cartilage invasion. *Arthritis & Rheumatism*. 2001; 44:676–681. [PubMed: 11263783]
16. Scott DL, Kingsley GH. Tumor necrosis factor inhibitors for rheumatoid arthritis. *N Engl J Med*. 2006; 355:704–712. [PubMed: 16914706]
17. Cohen S, Hurd E, Cush J, Schiff M, Weinblatt ME, Moreland LW, Kremer J, Bear MB, Rich WJ, McCabe D. Treatment of rheumatoid arthritis with anakinra, a recombinant human interleukin-1 receptor antagonist, in combination with methotrexate: results of a twenty-four-week, multicenter, randomized, double-blind, placebo-controlled trial. *Arthritis & Rheumatism*. 2002; 46:614–624. [PubMed: 11920396]
18. Cohen SB, Moreland LW, Cush JJ, Greenwald MW, Block S, Shergy WJ, Hanrahan PS, Khraishi MM, Patel A, Sun G, Bear MB. 990145 Study Group. A multicentre, double blind, randomised,

placebo controlled trial of anakinra (Kineret), a recombinant interleukin 1 receptor antagonist, in patients with rheumatoid arthritis treated with background methotrexate. *Annals of the Rheumatic Diseases*. 2004; 63:1062–1068. [PubMed: 15082469]

19. Maini RN, Taylor PC, Szechinski J, Pavelka K, Bröll J, Balint G, Emery P, Raemen F, Petersen J, Smolen J, Thomson D, Kishimoto T. Double-blind randomized controlled clinical trial of the interleukin-6 receptor antagonist, tocilizumab, in European patients with rheumatoid arthritis who had an incomplete response to methotrexate. *Arthritis & Rheumatism*. 2006; 54:2817–2829. [PubMed: 16947782]
20. Emery P, Keystone E, Tony HP, Cantagrel A, van Vollenhoven R, Sanchez A, Alecock E, Lee J, Kremer J. IL-6 receptor inhibition with tocilizumab improves treatment outcomes in patients with rheumatoid arthritis refractory to anti-tumour necrosis factor biologicals: results from a 24-week multicentre randomised placebo-controlled trial. *Annals of the Rheumatic Diseases*. 2008; 67:1516–1523. [PubMed: 18625622]
21. Prince FHM, Bykerk VP, Shadick NA, Lu B, Cui J, Frits M, Iannaccone CK, Weinblatt ME, Solomon DH. Sustained rheumatoid arthritis remission is uncommon in clinical practice. *Arthritis Research & Therapy*. 2012; 14:R68. [PubMed: 22429277]
22. Schwartz DM, Bonelli M, Gadina M, O’Shea JJ. Type I/II cytokines, JAKs, and new strategies for treating autoimmune diseases. *Nat Rev Rheumatol*. 2016; 12:25–36. [PubMed: 26633291]
23. Lindstrom TM, Robinson WH. A Multitude of Kinases-Which are the Best Targets in Treating Rheumatoid Arthritis? *Rheumatic Disease Clinics of NA*. 2010; 36:367–383.
24. Genovese MC, Kavanaugh A, Weinblatt ME, Peterfy C, DiCarlo J, White ML, O’Brien M, Grossbard EB, Magilavy DB. An oral Syk kinase inhibitor in the treatment of rheumatoid arthritis: a three-month randomized, placebo-controlled, phase II study in patients with active rheumatoid arthritis that did not respond to biologic agents. *Arthritis & Rheumatism*. 2011; 63:337–345. [PubMed: 21279990]
25. Arthur JSC, Ley SC. Mitogen-activated protein kinases in innate immunity. *Nat Rev Imm*. 2013; 13:679–692.
26. Matthew SG, Hayden S. NF- κ B in immunobiology. *Cell Research*. 2011; 21:223–244. [PubMed: 21243012]
27. Hanada T, Yoshimura A. Regulation of cytokine signaling and inflammation. *Cytokine & Growth Factor Reviews*. 2002; 13:413–421. [PubMed: 12220554]
28. Taylor PC, Feldmann M. Anti-TNF biologic agents: still the therapy of choice for rheumatoid arthritis. *Nat Rev Rheumatol*. 2009; 5:578–582. [PubMed: 19798034]
29. Gibbons LJ, Hyrich KL. Biologic Therapy for Rheumatoid Arthritis. *BioDrugs*. 2009; 23:111–124. [PubMed: 19489652]
30. Nah SS, Won HJ, Ha E, Kang I, Cho HY, Hur SJ, Lee SH, Baik HH. Epidermal growth factor increases prostaglandin E2 production via ERK1/2 MAPK and NF- κ B pathway in fibroblast like synoviocytes from patients with rheumatoid arthritis. *Rheumatol Int*. 2009; 30:443–449. [PubMed: 19680656]
31. Niepel M, Hafner M, Pace EA, Chung M, Chai DH, Zhou L, Muhlich JL, Schoeberl B, Sorger PK. Analysis of growth factor signaling in genetically diverse breast cancer lines. *BMC Biol*. 2014; 12:20. [PubMed: 24655548]
32. Alexopoulos LG, Saez-Rodriguez J, Cosgrove BD, Lauffenburger DA, Sorger PK. Networks inferred from biochemical data reveal profound differences in toll-like receptor and inflammatory signaling between normal and transformed hepatocytes. *Mol Cell Proteomics*. 2010; 9:1849–1865. [PubMed: 20460255]
33. Duvenaud DK, Eaton D, Murphy KP, Schmidt M. Causal learning without DAGs. *J Mach Learn Res Workshop Conf Proc*. 2010; 6:177–190.
34. Benjamini Y, Hochberg Y. Controlling the FDR- practical and powerful approach to multiple testing. *Journal of the Royal Statistical Society Series B*. 1995; 57:289–300.
35. Wajant H, Pfizenmaier K, Scheurich P. Tumor necrosis factor signaling. *Cell Death Differ*. 2003; 10:45–65. [PubMed: 12655295]
36. Davies SP, Reddy H, Caivano M, Cohen P. Specificity and mechanism of action of some commonly used protein kinase inhibitors. *Biochem J*. 2000; 351:95–105. [PubMed: 10998351]

37. Selness SR, Devraj RV, Devadas B, Walker JK, Boehm TL, Durley RC, Shieh H, Xing L, Rucker PV, Jerome KD, Benson AG, Marrufo LD, Madsen HM, Hitchcock J, Owen TJ, Christie L, Promo MA, Hickory BS, Alvira E, Naing W, Blevis-Bal R, Messing D, Yang J, Mao MK, Yalamanchili G, Vonder Embse R, Hirsch J, Saabye M, Bonar S, Webb E, Anderson G, Monahan JB. Discovery of PH-797804, a highly selective and potent inhibitor of p38 MAP kinase. *Bioorganic & Medicinal Chemistry Letters*. 2011; 21:4066–4071. [PubMed: 21641211]
38. de la Fuente A, Bing N, Hoeschele I, Mendes P. Discovery of meaningful associations in genomic data using partial correlation coefficients. *Bioinformatics*. 2004; 20:3565–3574. [PubMed: 15284096]
39. Zhang T, Inesta-Vaquera F, Niepel M, Zhang J, Ficarro SB, Machleidt T, Xie T, Marto JA, Kim N, Sim T, Laughlin JD, Park H, LoGrasso PV, Patricelli M, Nomanbhoy TK, Sorger PK, Alessi DR, Gray NS. Discovery of potent and selective covalent inhibitors of JNK. *Chem Biol*. 2012; 19:140–154. [PubMed: 22284361]
40. Davis MI, Hunt JP, Herrgard S, Ciceri Pietro, Wodicka LM, Pallares G, Hocker M, Treiber DK, Zarrinkar PP. Comprehensive analysis of kinase inhibitor selectivity. *Nature Biotechnology*. 2011; 29:1046–1051.
41. Overall JE, Rhoades HM. Beware of a half-tailed test. *Psychological Bulletin*. 1986; 100:121–122. [PubMed: 3737790]
42. Ronald, AF. *Statistical methods for research workers*. Edinburgh: Oliver and Boyd; 1925.
43. Junttila MR, Li SP, Westermarck J. Phosphatase-mediated crosstalk between MAPK signaling pathways in the regulation of cell survival. *FASEB J*. 2008; 22:954–965. [PubMed: 18039929]
44. Fey D, Croucher DR, Kolch W, Kholodenko BN. Crosstalk and signaling switches in mitogen-activated protein kinase cascades. *Front Physiol*. 2012; 3:355. [PubMed: 23060802]
45. Sichani MF, Moerke NJ, Niepel M, Zhang T, Gray NS, Sorger PK. Systematic analysis of BRAFV600E melanomas reveals a role for JNK/c-Jun pathway in adaptive resistance to drug-induced apoptosis. *Mol Syst Biol*. 2015; 11:797–797. [PubMed: 25814555]
46. Junttila MR, Li SP, Westermarck J. Phosphatase-mediated crosstalk between MAPK signaling pathways in the regulation of cell survival. *FASEB J*. 2008; 22:954–965. [PubMed: 18039929]
47. Staples CJ, Owens DM, Maier JV, Cato ACB, Keyse SM. Cross-talk between the p38alpha and JNK MAPK pathways mediated by MAP kinase phosphatase-1 determines cellular sensitivity to UV radiation. *J Biol Chem*. 2010; 285:25928–25940. [PubMed: 20547488]
48. Casals Casas C, Álvarez E, Serra M, de la Torre C, Farrera C, Sánchez Tilló E, Caelles C, Lloberas J, Celada A. CREB and AP-1 activation regulates MKP-1 induction by LPS or M-CSF and their kinetics correlate with macrophage activation versus proliferation. *Eur J Immunol*. 2009; 39:1902–1913. [PubMed: 19585511]
49. Xiao YQ, Malcolm K, Worthen GS, Gardai S, Schiemann WP, Fadok VA, Bratton DL, Henson PM. Cross-talk between ERK and p38 MAPK mediates selective suppression of pro-inflammatory cytokines by transforming growth factor-beta. *Journal of Biological Chemistry*. 2002; 277:14884–14893. [PubMed: 11842088]
50. Molina G, Vogt A, Bakan A, Dai W, Queiroz de Oliveira P, Znosko W, Smithgall TE, Bahar I, Lazo JS, Day BW, Tsang M. Zebrafish chemical screening reveals an inhibitor of Dusp6 that expands cardiac cell lineages. *Nature Chemical Biology*. 2009; 5:680–687. [PubMed: 19578332]
51. Naqvi S, Macdonald A, McCoy CE, Darragh J, Reith AD, Arthur JSC. Characterization of the cellular action of the MSK inhibitor SB-747651A. *Biochem J*. 2012; 441:347–357. [PubMed: 21970321]
52. Cargnello M, Roux PP. Activation and function of the MAPKs and their substrates, the MAPK-activated protein kinases. *Microbiol Mol Biol Rev*. 2011; 75:50–83. [PubMed: 21372320]
53. Kahle P, Saal JG, Schaudt K, Zacher J, Fritz P, Pawelec G. Determination of cytokines in synovial fluids: correlation with diagnosis and histomorphological characteristics of synovial tissue. *Annals of the Rheumatic Diseases*. 1992; 51:731–734. [PubMed: 1616355]
54. Thomas SJ, Snowden JA, Zeidler MP, Danson SJ. The role of JAK/STAT signalling in the pathogenesis, prognosis and treatment of solid tumours. *Br J Cancer*. 2015; 113:365–371. [PubMed: 26151455]

55. Thiel MJ, Schaefer CJ, Lesch ME, Mobley JL, Dudley DT, Teclé H, Barrett SD, Schrier DJ, Flory CM. Central role of the MEK/ERK MAP kinase pathway in a mouse model of rheumatoid arthritis: potential proinflammatory mechanisms. *Arthritis & Rheumatism*. 2007; 56:3347–3357. [PubMed: 17907188]
56. Brasier AR. The NF- κ B regulatory network. *Cardiovasc Toxicol*. 2006; 6:111–130. [PubMed: 17303919]
57. Carmona-Rivera C, Carlucci PM, Moore E, Lingampalli N, Uchtenhagen H, James E, Liu Y, Bicker KL, Wahamaa H, Hoffmann V, Catrina AI, Thompson P, Buckner JH, Robinson WH, Fox DA, Kaplan MJ. Synovial fibroblast-neutrophil interactions promote pathogenic adaptive immunity in rheumatoid arthritis. *Sci Immunol*. 2017; 2:eaag3358. [PubMed: 28649674]
58. Avdi NJ, Malcolm KC, Nick JA, Worthen GS. A role for protein phosphatase-2A in p38 mitogen-activated protein kinase-mediated regulation of the c-Jun NH(2)-terminal kinase pathway in human neutrophils. *Journal of Biological Chemistry*. 2002; 277:40687–40696. [PubMed: 12186863]
59. Westermark J, Li SP, Kallunki T, Han J, Kähäri VM. p38 mitogen-activated protein kinase-dependent activation of protein phosphatases 1 and 2A inhibits MEK1 and MEK2 activity and collagenase 1 (MMP-1) gene expression. *Mol Cell Biol*. 2001; 21:2373–2383. [PubMed: 11259586]
60. Cheung PCF, Campbell DG, Nebreda ÁR, Cohen P. Feedback control of the protein kinase TAK1 by SAPK2a/p38alpha. *EMBO J*. 2003; 22:5793–5805. [PubMed: 14592977]
61. Gaestel M, Kotlyarov A, Kracht M. Targeting innate immunity protein kinase signalling in inflammation. *Nat Rev Drug Discov*. 2009; 8:480–499. [PubMed: 19483709]
62. Kremontsov DN, Thornton TM, Teuscher C, Rincon M. The emerging role of p38 mitogen-activated protein kinase in multiple sclerosis and its models. *Mol Cell Biol*. 2013; 33:3728–3734. [PubMed: 23897428]
63. Ngkelo A, Adcock IM. New treatments for COPD. *Current Opinion in Pharmacology*. 2013; 13:362–369. [PubMed: 23602653]
64. Bertrand MJ, Tardif JC. Inflammation and beyond: new directions and emerging drugs for treating atherosclerosis. *Expert Opin Emerg Drugs*. 2017; 22:1–26. [PubMed: 27927063]
65. Fisk M, Gajendragadkar PR, Mäki-Petäjä KM, Wilkinson IB, Cheriyan J. Therapeutic potential of p38 MAP kinase inhibition in the management of cardiovascular disease. *Am J Cardiovasc Drugs*. 2014; 14:155–165. [PubMed: 24504769]
66. Wang S, Ding L, Ji H, Xu Z, Liu Q, Zheng Y. The Role of p38 MAPK in the Development of Diabetic Cardiomyopathy. *Int J Mol Sci*. 2016; 17:1037.
67. Leung L, Cahill CM. TNF- α and neuropathic pain - a review. *Journal of Neuroinflammation*. 2010; 7:27. [PubMed: 20398373]
68. Lin X, Wang M, Zhang J, Xu R. p38 MAPK: A Potential Target of Chronic Pain. *Current medicinal chemistry*. 2014; 21:4405–4418. [PubMed: 25245374]
69. Rosengren S, Boyle DL, Firestein GS. Acquisition, culture, and phenotyping of synovial fibroblasts. *Methods Mol Med*. 2007; 135:365–375. [PubMed: 17951672]
70. Benjamini Y, Yekutieli D. The control of the false discovery rate in multiple testing under dependency. *Annals of statistics*. 2001; doi: 10.2307/2674075

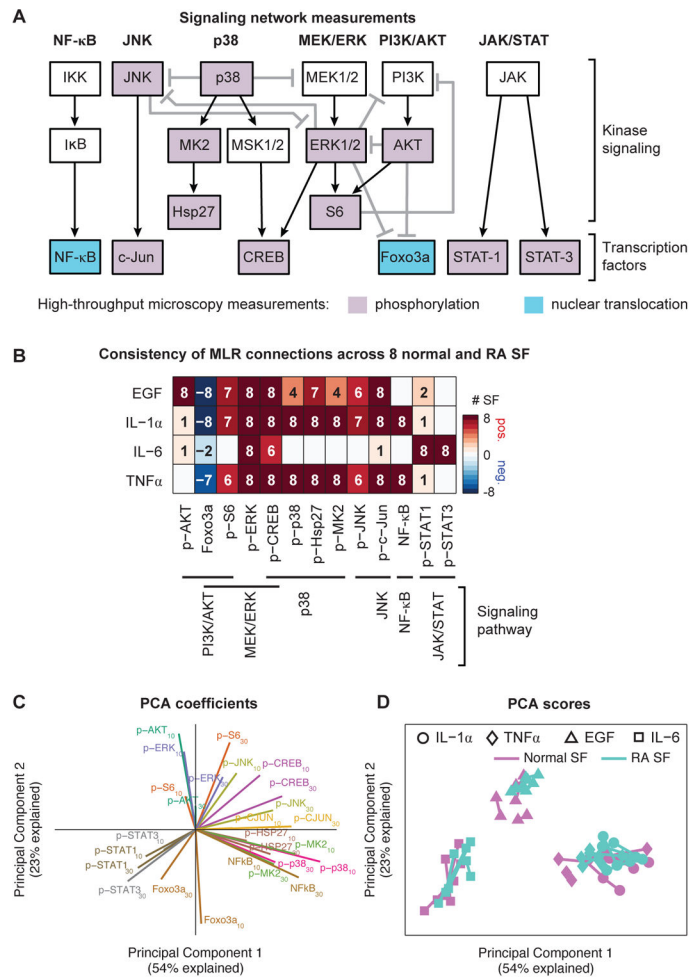


Figure 1. Consistent responses of normal and RA SF to inflammatory cytokines

(A) Simplified signaling network topology showing measured nodes and their relevant canonical signaling pathways. Activation was evaluated after 10 and 30 min stimulation with 100 ng/mL EGF, IL-6, TNF α , or IL-1 α in biological duplicate in four normal and four RA SF samples; a full experimental replicate was performed on separate days for a total of four replicates for each stimulus. (B) Summary of the activation of network proteins (columns) by the stimuli (rows) were categorized as positive or negative based on MLR β coefficients merged across experiments and time and counted across the eight SF samples (four normal and four RA). (C and D) Principal components analysis (PCA) of MLR β coefficients for the network proteins. PCA coefficients (C) for different time points of a given signaling protein are shown in the same color. PCA scores (D) for MLR coefficients for a given stimuli and SF sample in the two experimental replicates are connected by a line.

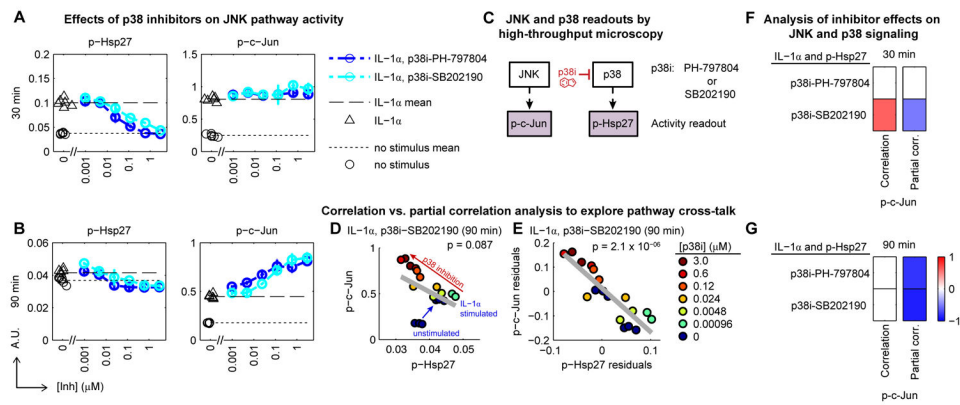


Figure 2. Enhancement of JNK signaling by p38 inhibition

(A to C) Perturbational strategy and dose response data for evaluation of two specific p38 inhibitors on c-Jun and Hsp27 phosphorylation (and thus, activation) after 30 or 90 min stimulation with IL-1 α (100 ng/mL). Serial five-fold dilutions of inhibitor (0.00096 to 3 μ M) were performed in biological duplicate in RA SF sample RA2159. Data are mean \pm S.D. (D) Pearson correlation between p-Hsp27 and p-c-Jun for the 90-min time point and p38 inhibitor SB202190. (E) Partial correlation analysis of p-c-Jun and p-Hsp27: correlation between the p-c-Jun and p-Hsp27 residuals after controlling for the effect of IL-1 α on p-Hsp27 and on p-c-Jun using MLR. (F and G) The correlation and partial correlation frameworks in D and E are applied to the data for both p38 inhibitors at the 30-min (F) or 90-min (G) time points. Partial correlations in (F and G), with $q_{BH} = 0.05$, were set to 0. A.U., arbitrary fluorescence units.

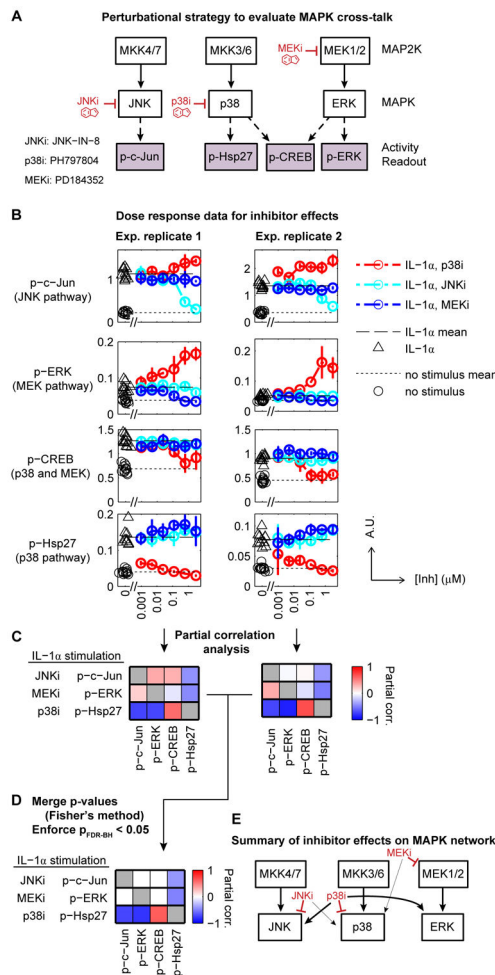


Figure 3. Dominant role for p38 in crosstalk between the MAPK pathways p38, JNK, and MEK in SFs

(A) Perturbational strategy for evaluating MAPK crosstalk. (B) Dose response data for specific p38, JNK, or MEK inhibitors after 90 min stimulation with IL-1 α (100 ng/mL). Titration was performed in biological quadruplicate on SF sample RA2159 and a full experimental replicate was repeated on a separate day (left vs. right). A.U., arbitrary fluorescence units. (C) Experimental replicates were individually evaluated for partial correlation between inhibitor effect (rows) and MAPK signaling (columns) while controlling for the primary effect of IL-1 α . Relevant proximal signaling measurements were used as a proxy to monitor canonical signaling downstream of a given inhibitor (for example, p-c-Jun was used as a surrogate for JNK pathway activity in the presence of the JNK inhibitor, p-ERK for MEK inhibition, and p-Hsp27 for p38 inhibition). “Self” partial correlation was excluded from the analysis (such as partial correlation between p-Hsp27 and p-Hsp27) and is shown in gray. (D) P-values and partial correlations from the independent experiments were merged using a modified Fisher’s method to allow for meta-analysis of two sided p-values (41, 42); partial correlations with q_{BH} (for the merged Fisher p-values) < 0.05 are set to 0. (E) Network summary of inferred inhibitor effects on MAPK signaling.

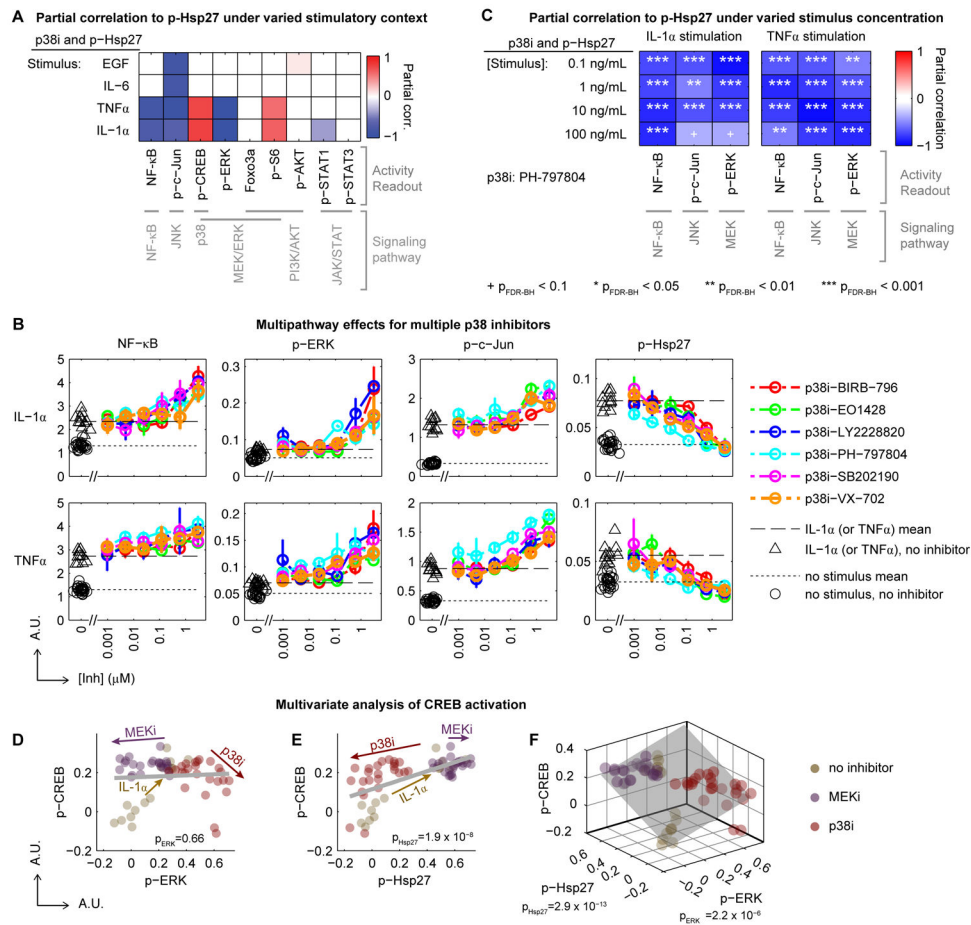


Figure 4. Network-wide analysis of cross-talk by p38

(A) Partial correlation between p-Hsp27 (as a handle for p38 pathway activity; rows) and network proteins (columns) conferred by p38 inhibition. Signaling network activity was evaluated after 90 min stimulation with EGF, IL-6, TNF α , or IL-1 α (each 100 ng/mL). Two experiments were performed on separate days on SF sample RA2159, with experiment 1 comprising titration of p38 inhibitor PH-797804 in biological duplicate and experiment 2 comprising 4–6 replicates of a single concentration of PH-797804 (0.6 μ M). P-values for the independent experimental replicates were merged using the modified Fisher's method (41, 42) and partial correlations with $q_{BH} = 0.05$ were set to 0. (B) Enhancement of NF κ B, ERK, and c-Jun activation in SF sample RA2159 after 90 min stimulation with IL-1 α or TNF α (each 100 ng/mL) by each of six p38 inhibitors, including four that were unsuccessfully evaluated in clinical trials for RA (BIRB-796, LY2228820, PH-797804, and VX-702). A.U., arbitrary fluorescence units. (C) Multipathway effects of PH-797804 across a concentration range (0.1 to 100 ng/mL) of IL-1 α and TNF α . (D to F) Reanalysis of MEK- and p38-inhibitor (MEKi and p38i) data from Fig. 3; univariate (D and E) and multivariate (F) analyses of correlations between p-ERK or p-Hsp27, and p-CREB.

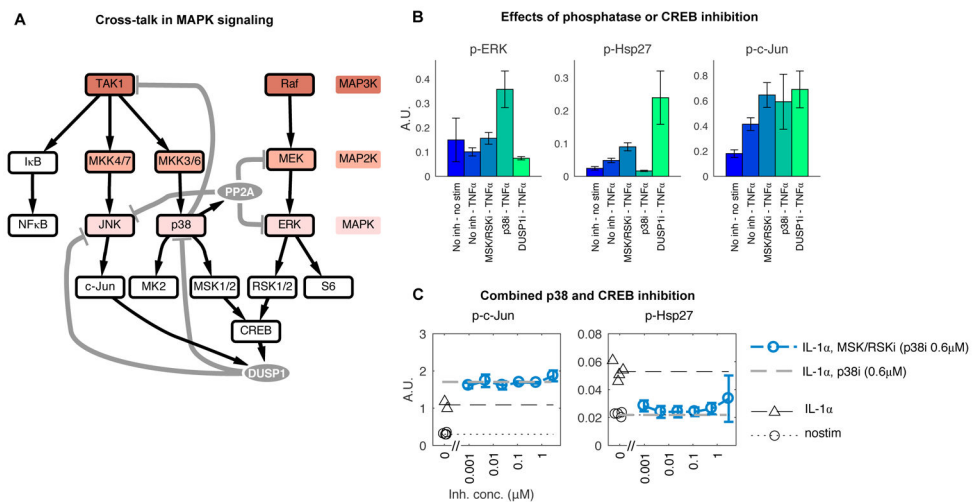


Figure 5. Exploring MAPK regulation and cross-talk in SF

(A) Schematic depicting MAPK signaling and cross-talk. Phosphatases are shown as gray ovals and negative regulatory feedback is shown as gray lines. (B) Effects of specific inhibitors of MSK/RSK (SB747651A; 3 μ M), or DUSP1 (BCI; 3 μ M) on MAPK signaling after 90 min stimulation with TNF α (100 ng/mL). MSK1/2 and RSK1/2 are respective p38- and MEK-dependent proximal upstream regulators of CREB. The p38 inhibitor PH-7978004 (0.6 μ M) was used for comparison. (C) Effects of MSK/RSKi and p38i combination on c-Jun and Hsp27 phosphorylation after 90 min stimulation. A.U., arbitrary fluorescence units.

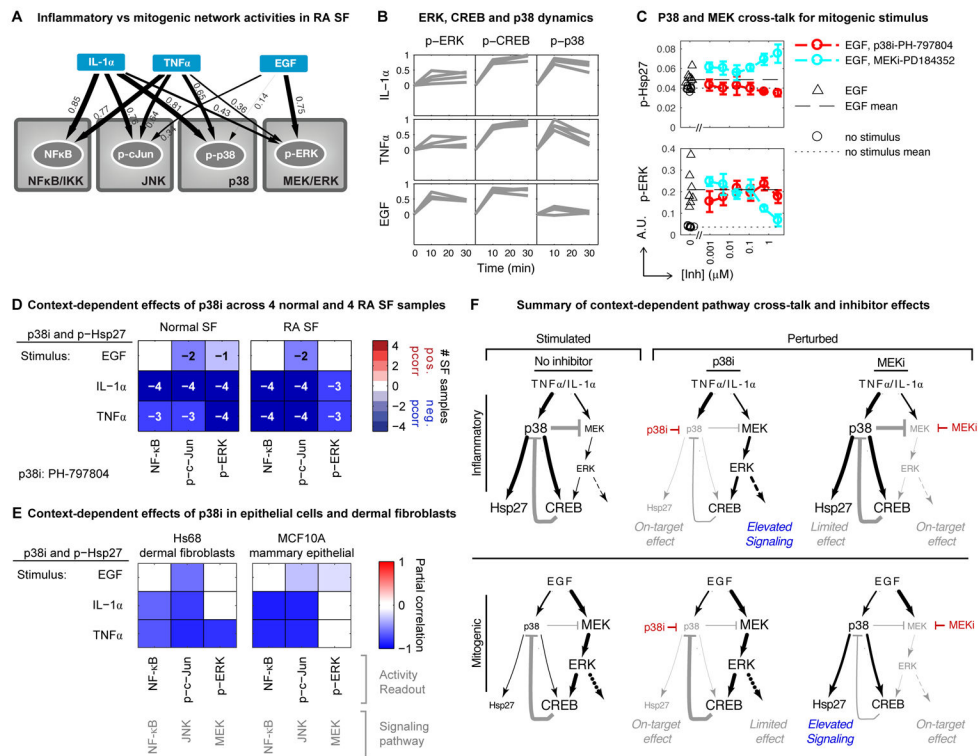


Figure 6. Inflammatory versus mitogenic stimulatory context-dependence of p38 and MEK inhibitors

(A) Node-edge graph of selected β coefficients from Fig. 1 (and Fig. S5) showing relative magnitudes of pathway activation by TNF α , IL-1 α , or EGF. Edge thickness is proportional to strength of MLR β coefficients that were averaged across time and RA SF sample for each node. (B) β coefficients of p-ERK, p-CREB, and p-p38 for RA SF samples plotted as a time course. Coefficients were scaled to a maximum of 1 for each node across all time points, SF samples, stimuli, and experimental replicates. (C) Effects of p38 or MEK inhibition on EGF-induced signaling in SF sample RA2159 (after 90 min incubation with 100 ng/mL EGF). (D) Partial correlation to p-Hsp27 across four normal or four RA SF samples; showing consistent context-dependent multipathway effects for p38 inhibition across SF samples. Nuclear translocation (for NF κ B) or phosphorylation was measured after 90 min stimulation with EGF, IL-1 α , or TNF α (100 ng/mL). (E) Partial correlation to p-Hsp27 for EGF, IL-1 α , or TNF α stimulation (100 ng/mL each for 90 min) in Hs68 dermal fibroblasts (left) or MCF10A mammary epithelial cells (right), showing similar context-dependence to that observed in SF samples. Hs68 or MCF10A cells were treated in biological quadruplicate and the full experiment was repeated across separate days. P-values for the independent experimental replicates were merged using the modified Fisher's method (41, 42) and partial correlations with $q_{BH} = 0.05$ were set to 0. (F) Schematic summarizing p38 and MEK inhibitor effects in inflammatory vs mitogenic contexts.

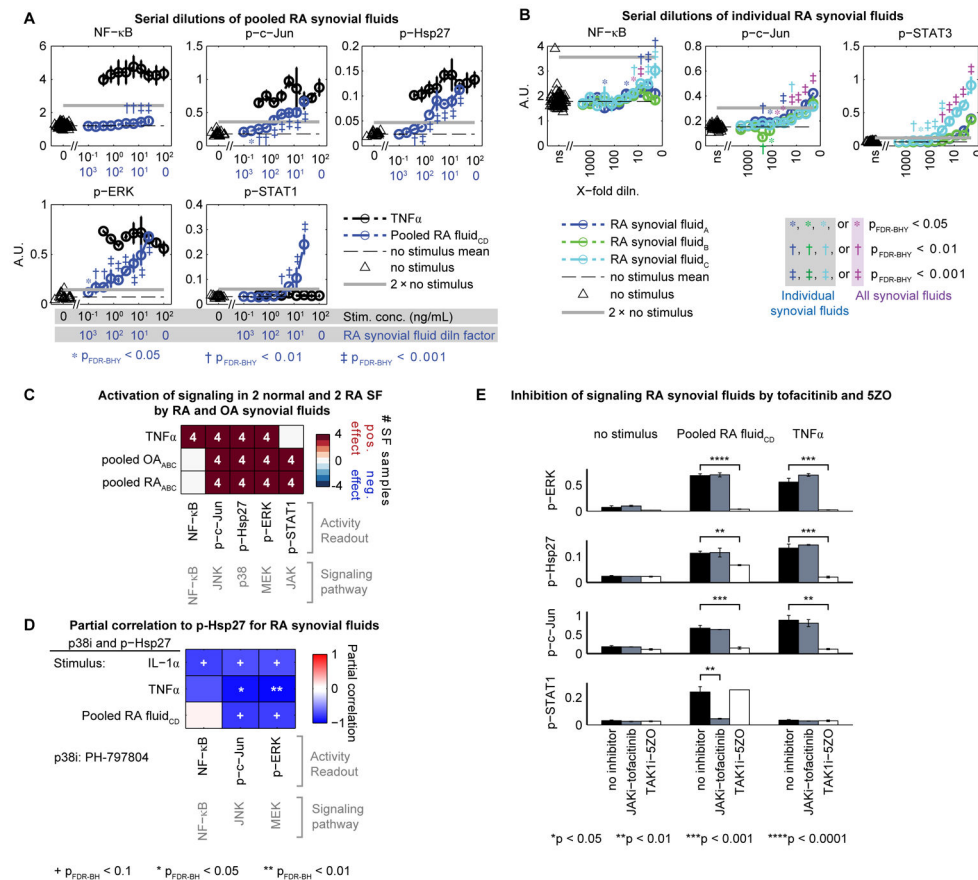


Figure 7. Activation of SF signaling by RA synovial fluids

(A) Activation of signaling in SFs by serial two-fold dilution of pooled RA synovial fluids into basal SF media (1:4 – 1:1024 dilution series of an equal volume mixture of RA fluid samples C and D); serial two-fold dilution of TNF α (0.4 – 100 ng/mL) was used as a positive control for NF κ B (nuclear translocation), p-c-Jun, p-Hsp27, and p-ERK. Data are mean \pm S.D. (B) Serial two-fold dilution of individual RA synovial fluid samples A, B, and C (1:2 – 1:2048 dilution series). (C) Consistency of signaling activation across two normal and two RA SF samples (as determined by MLR analyses) by 1:4 dilution of pooled RA synovial fluids (equal volumes of RA fluid samples A, B, and C) or pooled OA synovial fluids (equal volumes of OA fluid samples A, B, and C). (D) Partial correlation analysis for p38 inhibition augmenting signaling induced by pooled RA synovial fluids. (E) Effects of tofacitinib (1.5 μ M) or 5ZO (1.0 μ M) on signaling induced by 1:4 dilution of pooled RA synovial fluids (30 min stimulation with equal volume mixture of RA synovial fluid samples C and D). TNF α (100 ng/mL) was used as a positive control. Data are mean \pm S.D. Signals were measured in biological duplicate after 30 min (A to C) or 90 min (D) stimulation in SF sample RA2159 (A, B, D, and E) or samples N2586, N2759, RA2159, and RA2708 (C). Significance was determined by an unpaired two-sample Student’s t-test (synovial fluid dilutions vs. unstimulated signal; A and B); false discovery rate was controlled using the Benjamini-Hochberg-Yekutieli method for positive dependence (q_{BHY}) (70).